Effect of temperature on the modal parameters of continuous rigid frame bridge

Developments in the Built Environment 21 (2025) 100631

Contents lists available at ScienceDirect

Developments in the Built Environment

journal homepage: www.sciencedirect.com/journal/developments-in-the-built-environment

Effect of temperature on the modal parameters of continuous rigid frame bridge

Yang Yang [a,b,*], Md Sulayman Hossen [a,b], Giuseppe Lacidogna [c], Wenming Xu [a,b], Ibna Kawsar [d], Junbo Sun [b], Shameem Hossain [e]

[a] School of Civil Engineering, Chongqing University, Chongqing, 400030, China
[b] Institute for Smart City of Chongqing University in Liyang, Chongqing University, Jiangsu, 213300, China
[c] Department of Structural, Geotechnical and Building Engineering, Politecnico di Torino, 10129, Torino, Italy
[d] School of Mechanical and Vehicle Engineering, Chongqing University, Chongqing, 400044, China
[e] Department of Bridge Engineering, College of Civil Engineering, Tongji University, Shanghai, 200092, China

ARTICLE INFO

Keywords:
Temperature effect
Modal parameters
Continuous rigid frame bridge
Structural health monitoring (SHM)

ABSTRACT

The temperature effect on modal parameters such as natural frequencies, mode shapes, and damping ratios is critical for precisely determining the health of a bridge. This is the first study investigating how temperature affects the modal properties of a large continuous rigid-frame bridge. The vibration experiment data was collected and analyzed 39 times within a year's maximum and minimum temperatures. The frequency has been analyzed using the Fast Fourier transform (FFT) algorithm. Mode shape and damping ratio were analyzed using MATLAB software using the covariance-driven stochastic subspace identification method (SSI-COV) and the logarithmic decrement method. Due to the unique shape of the bridge, numerical simulations were performed using Midas Civil software to validate the results. Moreover, the correlation coefficients of frequencies and damping ratios at different temperatures have been evaluated by this observation, which will assist in identifying the large continuous rigid frame bridge's health at various temperatures.

1. Introduction

Over the past three decades, bridge construction has advanced quickly due to continuing developments in science and technology (Abdal et al., 2023). In recent years, the number of bridges worldwide equipped with structural health monitoring (SHM) systems has increased (Liu, 2023). Bridges are expensive, complex structures that last for many years. However, each bridge ages differently and requires different maintenance at different times. Zhu et al. (2023) noticed that early detection of potential damage is essential to maintaining the bridge's safety and enhancing its management and maintenance effectiveness. There are many techniques around the world to detect structural damage. Bai et al. (2023) categorized two primary structural damage detection techniques: vibration-based and static-based. Vibration-based detection techniques are becoming more common in civil engineering, aircraft, manufacturing, and other fields as technology advances (Dang et al., 2022). One kind of worldwide monitoring is called vibration-based monitoring, or VBM (Brownjohn et al., 2011). The foundation is the relationship between a structure's mass, energy dissipation, stiffness, and dynamic behavior. J. J. Moughty and J. R. Casas (Moughty and Casas, 2017) observed that these factors are all dictated by the structure's modal properties, including natural frequencies, mode shapes, and damping ratios.

The impact of temperature fluctuations on the modal characteristics of bridges, such as natural frequencies, mode shapes, and damping ratios, has been the subject of several studies. Luo et al. (2022) studied the impact of temperature fluctuations on natural frequencies and (Xia et al., 2012) reviewed the effects of temperature fluctuations on mode shapes. Wang et al. (2020) investigated the effect of temperature on the damping ratio of a structure. A crucial area of structural engineering is the behavior of bridges under temperature variations, as researched (Xia et al., 2022). The bridge's total reaction is greatly influenced by its modal properties, so it is essential to justify its dynamic response to temperature variations. The natural frequency of bridge structures is a critical parameter in the design (Akbari et al., 2018), detection, and damage identification (Mekjavić, 2013). Several studies indicate that

* Corresponding author. School of Civil Engineering, Chongqing University, Chongqing, 400030, China.
E-mail addresses: yangyangcqu@cqu.edu.cn (Y. Yang), l2200016@stu.cqu.edu.cn (M.S. Hossen), giuseppe.lacidogna@polito.it (G. Lacidogna), 20211601028@cqu.edu.cn (W. Xu), l2200089@stu.cqu.edu.cn (I. Kawsar), tunneltc@gmail.com (J. Sun), 2293331@tongji.edu.cn (S. Hossain).

https://doi.org/10.1016/j.dibe.2025.100631
Received 7 December 2024; Received in revised form 16 February 2025; Accepted 23 February 2025
Available online 24 February 2025

temperature variations can affect the frequency (Salawu, 1997), and Kim et al. (2007) observed sometimes covering structural damage. So, a complete understanding of the effect of temperature is necessary for accurate structural health monitoring (SHM).

More recent studies have focused on the impact of temperature on the modal analysis of large bridges. A paper by (Chalouhi et al., 2018) introduces a machine-learning approach that detects damage in steel railway bridges, accounting for temperature variations. The algorithm uses Artificial Neural Networks (ANNs) to predict deck accelerations during train passages under undamaged conditions, comparing these predictions with real measurements. The study found that neglecting temperature reduced prediction accuracy, emphasizing the need to consider environmental factors in damage assessment. Another recent study conducted by (Borlenghi et al., 2024) highlights the operational modal testing and finite element model updating of a masonry bridge. This research, using a historical masonry viaduct as a case study, stresses the importance of accurate methodologies in structural health monitoring (SHM) and shows how low temperatures affect experimental data reliability by establishing a relationship between Young's modulus and air temperature, leading to increased natural frequencies below 0 °C.

To properly identify the health of the structures, scholars have been researching how the modal properties are affected by environmental factors. Most researchers have been working on small structures because of limitations, such as weather, laboratories, instruments, time-consuming, etc. The effect of temperature on the modal frequency of a concrete beam using field monitoring data has been studied, and it has been noticed that the effect of temperature on the frequency is remarkable (Shan et al., 2018). Wang et al. (2020) worked on the effects of temperature on vibration-based damage detection in a reinforced concrete slab. Temperature influences the modal properties of a simply supported beam bridge (He et al., 2022). The temperature influences the daily modal variability of a steel-concrete composite bridge has been studied, though it has not mentioned damping ratio and mode shape (Mosavi et al., 2012). The impact of temperature on the modal properties without the practical mode shape of a cable-stayed bridge has been investigated(Asadollahi and Li, 2017). Other research examines the influence of temperature on only modal frequencies in a continuous rigid frame bridge through extended observation (Wang et al., 2011), however, this bridge is not fully rigid with all piers. Most of the research has been on the temperature effect on the frequency of small structures, there are few studies in the literature that explicitly establish correlations between temperature variations and bridge modal parameters.

No research has justified the FE results with practical results on the effect of temperature on three modal parameters together of a continuous rigid frame bridge. So, for a clear understanding of the effect of temperature on modal parameters such as natural frequency, mode shape, and damping ratio of a large bridge structure, this study has observed one year and collected data from an existing large continuous rigid frame bridge. This study has created a novel correlation between the natural frequencies, damping ratios, and temperature, as well as shown the mode shapes at different temperatures of a continuous rigid-frame bridge. Additionally, it has evaluated the correlation coefficient of frequencies and damping ratios at different temperatures in various environments, which will facilitate accurately detecting the health of such bridges. Temperature and damage are pronounced factors that influence the modal parameters. However, several factors also might change the modal parameters of a structure for example Changing boundary conditions (Shi et al., 2019), changing material properties due to e.g. hardening of concrete (Magalhães et al., 2009), etc. Additionally, This study mainly focused on the impact of temperature on the modal parameters of the bridge. Future studies might consider all the factors that impact the modal parameters of a structure for precise results. Without understanding the effect of temperature variation on a continuous rigid-frame bridge, it is challenging precisely to identify the bridge's health.

2. Theoretical temperature effects on modal parameters

2.1. Temperature's effect on elastic modulus, length, and moment of inertia of the concrete structure

One of the important influence factors that need to be measured is the temperature effect on the elastic modulus of concrete. Concrete is a temperature-sensitive material, and its stiffness and structural resistance, represented by the concrete's modulus of elasticity (E), are strongly influenced by temperature changes. The impact of temperature on the elastic modulus of concrete is more significant than the elastic modulus of steel bars. The primary component of the concrete structure is concrete. Therefore, the impact of temperature on the reinforcing bar was ignored. According to the calculation formula in the European Concrete Specification CEB-FIP Model Code, 2010 (Code, 2010), the effect of temperature on concrete elastic modulus was analyzed:

$$E_T = E_{20^\circ c}[1 - \theta_E(T - 20)], \tag{1}$$

where E_T represents the Elastic modulus (MPa) of concrete at T temperature. T is the temperature of concrete (∘C). $E_{20^\circ c}$ is the Elastic modulus of concrete (MPa) at 20 °C, room temperature. θ_E is the temperature coefficient of elastic modulus, with a value of 0.003.

Based on the temperature dependence of the concrete elasticity modulus referred to above, this section further explores its effect on the overall structural stiffness. As described by Cai et al. (2021), the authors identified the temperature effect on elastic modulus, moment of inertia, and the length of the concrete structure, and those parameters how much affect the modal frequency. The finding shows that the influence coefficient of the elastic modulus can be denoted as $\lambda_E = 1.08628$; while the influence coefficient of the moment of inertia can be described as $\lambda_I = 0.99976$. Additionally, $\lambda_l = 1.0012$ represents the beam length coefficient. Considering an ultimate cooling temperature of T = 60 °C, the elastic modulus of the simply supported beam results in a frequency increase of 8.628%. Conversely, changes in the moment of inertia lead to a frequency decrease of 0.024%, and the beam length causes an increase of 0.12%. The combined effect of structural size contributes to an overall frequency increase of 0.096%. Changes in the moment of inertia and beam length have minimal significance. The variation in the natural frequency of the simply supported beam with temperature is primarily associated with the material's elastic modulus, while structural size has little impact on frequency.

2.2. Temperature's effect on modal properties

The following Equation (2) expresses the motion equation of a structure:

$$[M]\ddot{x} + [C]\dot{x} + [K]x = \{f\}, \tag{2}$$

where $\ddot{x}$, $\dot{x}$, and x are vectors representing the accelerations, velocities, and displacements, and $[M]$, $[C]$, and $[K]$ are the mass, damping, and stiffness matrices for the bridge model, respectively, while $\{f\}$ is the external force.

The elementary beam element stiffness matrix $[Ke]$ is formulated using the Euler-Bernoulli beam theory as follows:

$$[Ke] = \frac{EI}{L^3}\begin{bmatrix} 12 & 6L & -12 & 6L \\ 6L & 4L^2 & -6L & 2L^2 \\ -12 & -6L & 12 & -6L \\ 6L & 2L^2 & -6L & 4L^2 \end{bmatrix}, \tag{3}$$

where $[Ke]$, E, and I represent the stiffness matrix, elastic modulus, and moment of inertia, respectively, and beam length is L. Note: In this article, $[K]$ is the global stiffness matrix, which can be the element stiffness matrix.

Then, as is well known, to calculate the global stiffness matrix $[K]$, the structure is divided into elements, each of which has its calculated

elemental stiffness [*Ke*]. The elements represent small portions of the structure's volume and are defined by the connection of various nodes where the system's degrees of freedom concentrate. In a structural problem, the degrees of freedom (DOF) typically include displacements and/or rotations, sometimes supplemented by pressures, strains, temperature variation, etc. Volume and surface forces are converted into equivalent nodal forces {*fe*}, calculated for each element. The elemental matrices and vectors are assembled into the global matrix [*K*] and the global vector {*f*}. The next step involves modifying the matrix [*K*] and vector {*f*} to account for boundary conditions (Doyle, 1991).

According to Equations (1)–(3), it is proven that temperature has a significant influence on modal parameters. Temperature changes the modulus of elasticity, the modulus of elasticity changes the stiffness, and finally, the stiffness changes the modal parameters.

For a simply supported uniform beam, the undamped flexural vibration frequency of order n is given below (Warburton et al., 1995):

$$f_n = \pi h \frac{n^2}{2l^2}\sqrt{\frac{E}{12\rho}}, \tag{4}$$

where n is the order of frequencies, h and l are the beam's height and length, and ρ and E are the beam materials' density and Young's modulus.

When a fixedly supported uniform beam swells and shrinks, it is confined at two ends. Therefore, it behaves similarly to a simply supported beam with axial force. Its n-order undamped flexural vibration frequency is given below (Xu et al., 2007):

$$f_n = \frac{n^2\pi}{2l^2}\sqrt{\frac{Eh^2}{12\rho} - \frac{Nl^2}{n^2\pi\rho bh}}, \tag{5}$$

where N represents the axial force, which is positive in compression. On a fixedly supported beam, the influence of temperature on modal frequencies is more complex because f_n depends on N, which indicates that restrictions impact it. Additionally, f_n is also dependent on h for this study; the value of h is unequal in different bridge positions because it is a continuous rigid frame bridge. Numerical simulation was used in this study to solve this problem.

Equation (6) has been developed to identify the natural frequencies of a continuous rigid frame bridge at different temperatures:

$$f_n(T) = c_n T + f_n, \tag{6}$$

where $f_n(T)$ is the n-order frequency of a continuous rigid frame bridge with respect to the temperatures. c_n, T, and f_n represent the temperature coefficient of natural frequency, temperature, and n-order natural frequency of a continuous rigid frame bridge, respectively.

The boundary conditions and structural characteristics of a bridge structure determine the equation for its mode shape. The general mode shape equations are as follows when material properties are uniform as described (De Luca et al., 2018).

The mode shapes of a simply supported beam are as follows:

$$\phi_n(x) = \sin\left(\frac{n\pi x}{L}\right), \tag{7}$$

where $\phi_n(x)$, n, and L represent the mode shape, order (1,2,3 ….), and bridge length.

The mode shapes of a n-span continuous rigid frame bridge are frequently described as follows:

$$\phi_n(x) = \sum_{i=1}^{n} A_i \sin\left(\frac{n\pi(x - L_{i-1})}{L_i}\right), \tag{8}$$

where $\phi_n(x)$ is the mode shape, each span's lengths are denoted by L_i, and the coefficients A_i are chosen based on the support conditions and continuity requirements.

Under the assumption of uniform material properties, the mode shapes of a simple supported beam and a multi-span continuous rigid frame bridge can be calculated from Equations (7) and (8), respectively. These equations are of common use in structural dynamics where material properties are almost the same over the structure. When different materials are used in other parts of the structure, or if the elastic modulus is significantly affected by the temperature at other locations, mode shapes may also be affected due to these alterations. In this study, the bridge model is studied in conditions in which temperature gradients and implications on the elastic modulus of different parts of the bridge are negligible. Because of its practical analysis, it is considered the average temperature of the bridge, so the effect of temperature on the modulus of elasticity is also the same along the bridge. Therefore the mode shapes are largely dictated by span lengths and boundary conditions, and any variation of material properties due to temperature variation may not have much effect on the results.

When discussing the free vibration response, the damping ratio might be represented in the natural frequency and the logarithmic decrement method:

$$\zeta = \frac{1}{2\pi}\frac{\delta}{\sqrt{1+\delta^2}}, \tag{9}$$

where δ is the logarithmic decrement, defined as:

$$\delta = \ln\left(\frac{x(t)}{x(t+T)}\right), \tag{10}$$

t is time, and T is the period of oscillation.

Equations (9) and (10) show that the damping ratio has a relation to the frequency. So, the damping ratio also has a temperature effect, although it is very tiny.

Equation (11) has been developed to identify the damping ratios of a continuous rigid frame bridge at different temperatures:

$$\zeta_n(\mathrm{T}) = c_n T + \zeta_n, \tag{11}$$

where $\zeta_n(\mathrm{T})$ is the n-order damping ratio of a continuous rigid frame bridge with respect to the temperatures. c_n, T and ζ_n represent the temperature coefficient of damping ratio, temperature, and n-order damping ratio of a continuous rigid frame bridge, respectively.

3. On-site bridge test verification

3.1. Descriptions of the bridge

The Sansheng Extra Large Bridge, located in Section HC03 of the Hechuan to Changshou segment of the Chongqing, China Third Ring Expressway, as shown in Fig. 1, is a prestressed concrete continuous rigid-frame bridge with a span composition of (80 + 3 × 150 + 80) m. The bridge decks have a total width of 12m, with an anti-collision guardrail arrangement of 0.5m + 11.0m (carriageway) + 0.5m (anti-collision guardrail).

The bridge is designed for the Class I loading level of the highway. The upper structure of the bridge box girder is a three-directional prestressed concrete structure with a concrete strength grade of C55, with low-relaxation high-strength steel wires. The main dimensions of the box girder are 12m top slab width, 6.5m bottom slab width, 9.3m beam height, and 3.3m midspan beam height. The central abutment of the lower structure is a double thin-wall hollow pier with a concrete strength grade of C40 and a cross-section size of 3.5m × 8.5m.

3.2. Sensor's setup of the bridge

Five accelerometers, Fig. 4 (a), have been set up specifically at the midpoint of every span of the bridge, as shown in Fig. 2. Accelerometers collected data in a vertical direction and were positioned in the lower sections of the box girder as shown in Fig. 3 (a). The positions of the

Fig. 1. The Sansheng Extra large bridge.

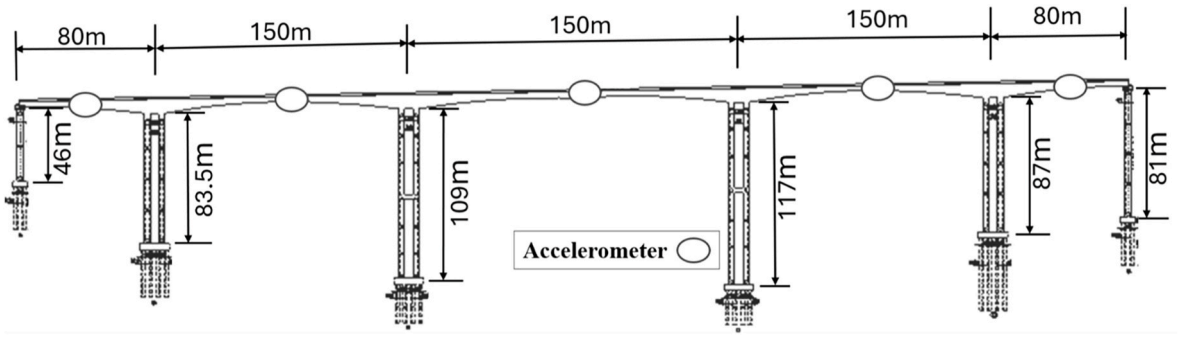

Fig. 2. Design of the investigated bridge and accelerometer's positions.

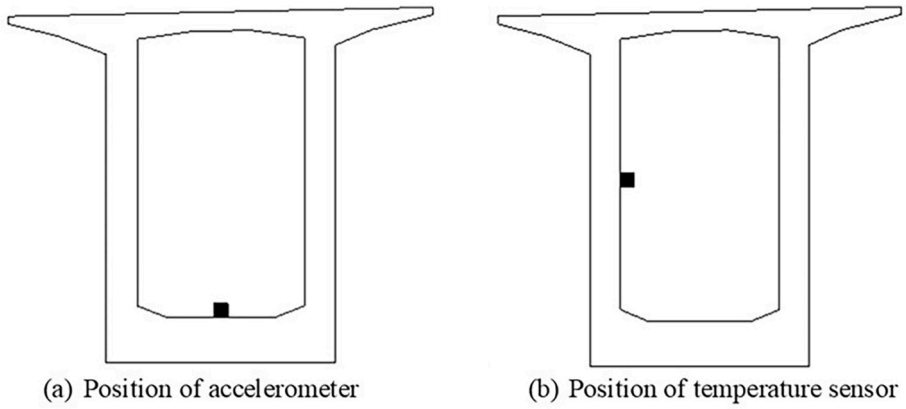

Fig. 3. Position of accelerometer and temperature sensor.

accelerometers were deliberately chosen to provide accurate results of the main vibration modes of the bridge.

The study considers the bridge temperature to be the inside temperature of the concrete. Temperature sensors are installed within the concrete, as illustrated in Fig. 4 (b), positioned on the side of the box girder, as shown in Fig. 3 (b). Temperatures within the structure are relatively consistent, with slight variations between the top and bottom parts of the box girder. The average temperature is primarily concentrated on the girder's side.

3.3. Data collection

This study has collected temperature data for 12 months, from August 2022 to August 2023, from the observation bridge cloud in the temperature data collecting window, as shown in Fig. 5 (b). The minimum and maximum temperatures ranged from 5 °C to 43 °C in one year. Then, 39 data points were selected from January 17, 2023, to August 12, 2023, because minimum and maximum temperatures were included in this range, as shown in Fig. 6. The acceleration data was obtained from these exact temperature data points from the observation bridge cloud in the acceleration window shown in Fig. 5(a).

3.4. Practical data analysis

3.4.1. Frequency

Five sets of experimental acceleration data were filtered using the

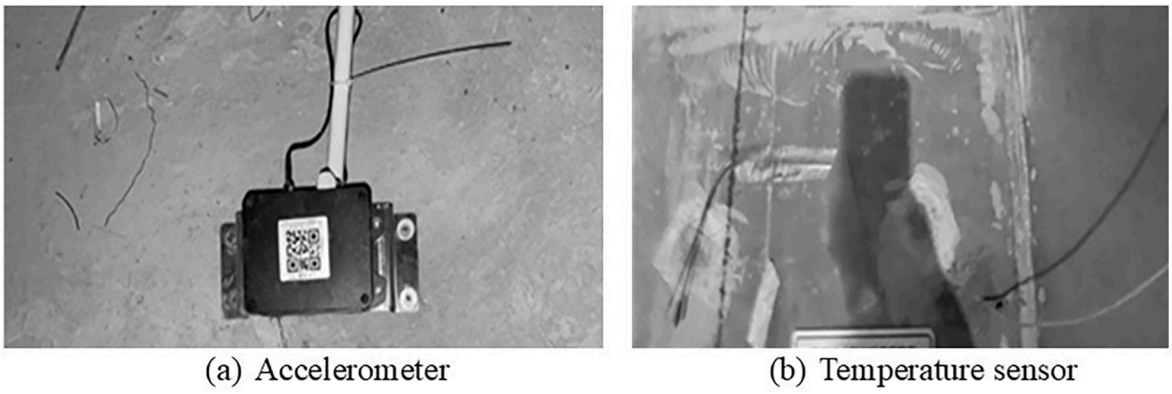

Fig. 4. Accelerometer and temperature sensor.

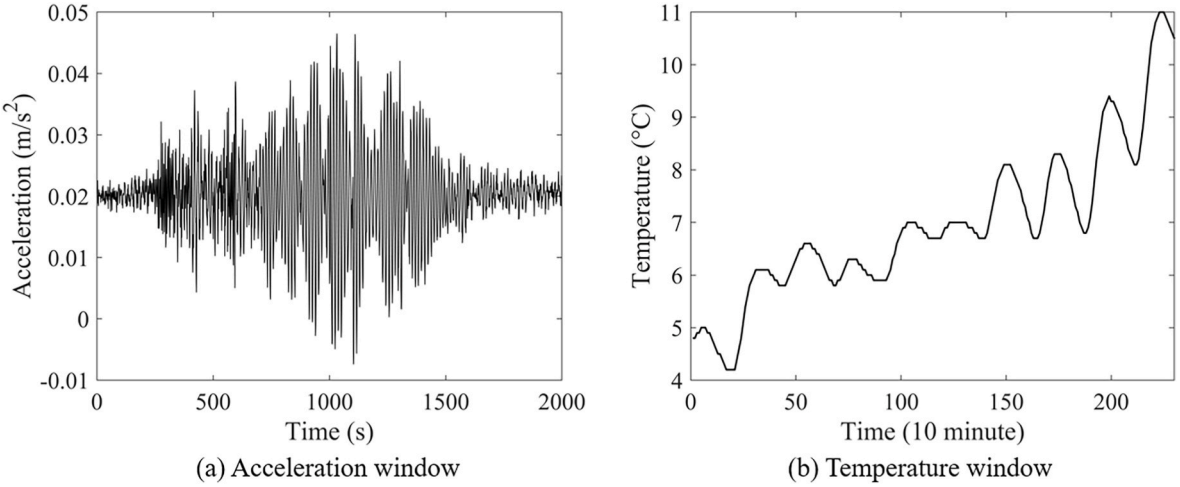

Fig. 5. The acceleration and temperature window.

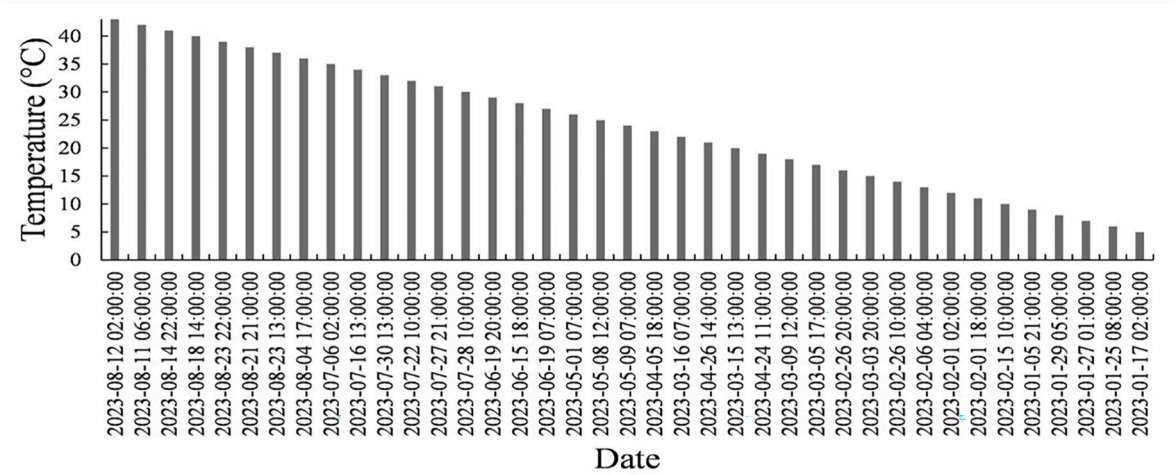

Fig. 6. Data collection in different temperatures.

bandpass filter and denoised using the wavelet denoiser. Then, acceleration data were analyzed using the Fast Fourier Transform (FFT) algorithm in MATLAB software to determine the frequency of the observation bridge. The five frequencies were statistically combined to calculate the bridge's average frequency. Moreover, linear regression was used to establish a correlation between the structure's temperature and frequency, which are described with points, as shown in Fig. 7. The equations of the fitted data have described the first, second, and third natural frequencies as $f_1(T) = -1.85 \times 10^{-3} \times T + 0.98$, $f_2(\mathrm{T}) = -1.83 \times 10^{-3} \times T + 1.27$, and $f_3(\mathrm{T}) = -2.01 \times 10^{-3} \times T + 1.49$, respectively. The correlation coefficients of the first, second, and third natural frequencies c_1, c_2, and c_3 are $= -1.85 \times 10^{-3}$, -1.83×10^{-3}, and -2.01×10^{-3}, showing a significant linear correlation between the temperature and the natural frequencies in the temperature range of

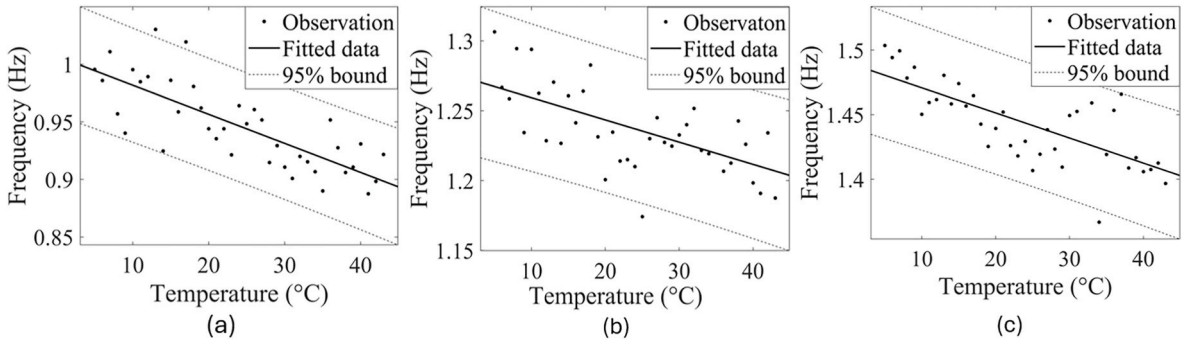

Fig. 7. Relationship between n-order (n = 1,2 and 3) a, b, and c, respectively, natural frequency and temperature of the practical results.

5 °C–43 °C. The observation with a 95% confidence interval is bounded with dotted lines, as shown in Fig. 7. As the temperature rises by one °C from 5 °C to 6 °C, the first-order natural frequency of 0.1893% decreases. The second and third-order natural frequencies also show a negative relationship with temperature. Reduces second-order and third-order frequency by 0.1442% and 0.1363%, respectively, when the temperature increases by 1 °C from 5 °C to 6 °C.

3.4.2. Mode shape

To accurately determine the mode shapes of the observation bridge, it is recognized that obtaining reliable signals from every accelerometer may not always be feasible. Therefore, this study has analyzed the first mode at six distinct temperatures: 10 °C, 15 °C, 20 °C, 25 °C, 30 °C, and 43 °C. Additionally, the second and third modes have been analyzed at different temperatures: 10 °C, 20 °C, 25 °C, 30 °C, and 43 °C, respectively, as shown in Fig. 8. Five sets of experimental acceleration data were filtered using the bandpass filter and denoised using the wavelet denoiser. Then, the SSI-COV (Stochastic Subspace Identification—Covariance) algorithm was employed using MATLAB software for mode shape analysis. The SSI-COV method is a powerful tool for modal analysis.

The result of the first mode shape demonstrated no changes at temperatures of 15 °C, 25 °C, and 43 °C, which proved that there is no temperature effect on the first mode shape as shown in Fig. 8 (a). Additionally, there are little changes at temperatures of 10 °C, 20 °C, and 30 °C; this might be the margin of error. The results of the second and third mode shapes are different at 10 °C, 20 °C, 25 °C, 30 °C, and 43 °C. So, it shows that the second and third mode shapes have a temperature effect, but it may be less than the margin of error, as shown in Fig. 8 (b) and (c).

However, detecting mode shapes of large structures that have complicated boundary conditions is challenging in practical work. There are several reasons why the results may not be fully accurate. Given the size and complexity of the bridge (610 m long continuous rigid frame), inherent variabilities in dynamic behavior were also discovered. As a highway, the traffic loads fluctuated a lot changing within the year over the different data measurement times. Moreover, variations in boundary conditions, caused by environmental reasons (i.e. temperature variations, or settlements) have an additional effect on mode shapes. Finally, the preprocessing of the data, such as filtering, denoising, and mode shape identification techniques process the data might also affect the mode shapes. All of these factors may cause a margin of error. To get an accurate result of temperature effect on the mode shape of a large structure, a large amount of tests are required.

3.4.3. Damping ratio

Five sets of experimental acceleration data were filtered using the bandpass filter and denoised using the wavelet denoiser. Then, acceleration data were analyzed using the logarithmic decrement method in MATLAB software to determine the damping ratio of the observation bridge. The damping ratios were statistically combined to calculate the bridge's average damping ratio. Moreover, linear regression was used to establish a correlation between the structure's temperature and damping ratio, which are described with points as observation damping ratio with a 95% confidence interval are bounded with dotted lines as shown in Fig. 9. The equations of the fitted data have described of the first, second, and third damping ratios are $\zeta_1(T) = -1.14 \times 10^{-6} \times T + 9.8 \times 10^{-4}$, $\zeta_2(T) = -2.1 \times 10^{-6} \times T + 3.9 \times 10^{-4}$, and $\zeta_3(T) = -8.4 \times 10^{-7} \times T + 2.9 \times 10^{-4}$, respectively. The temperature coefficients of the first, second, and third damping ratios c_1, c_2, and c_3 are -1.14×10^{-6}, -2.1×10^{-6}, and -8.4×10^{-7}. According to Fig. 9. The temperature effect on the damping ratio is minimal. As the temperature rises by one °C from 5 °C to 6 °C, the first-order damping ratio of $(7.7 \times 10^{-5})\%$ decreases. Second-order and third-order damping ratios show a negative relationship with temperature as well. Reduces second-order and third-order damping ratios by $(1.4 \times 10^{-4})\%$ and $(5.6 \times 10^{-5})\%$, respectively, when the temperature increases by 1 °C from 5 °C to 6 °C.

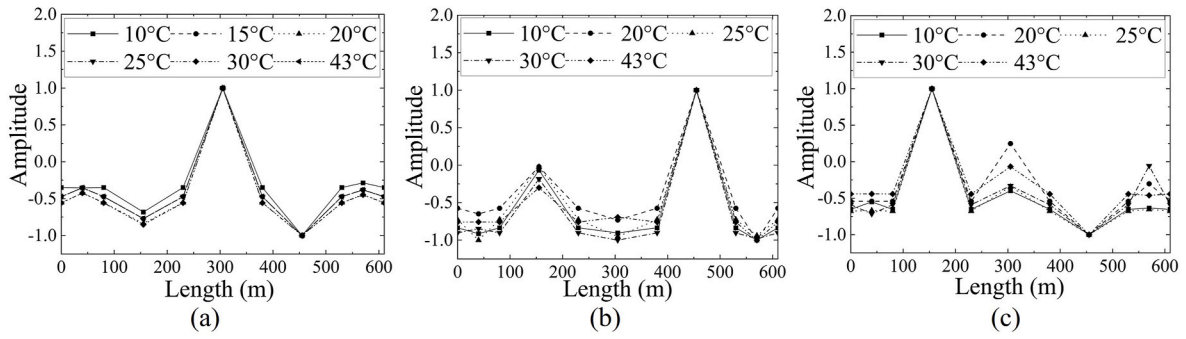

Fig. 8. The practical results of the first, second, and third modes (a, b, and c), respectively, at different temperatures.

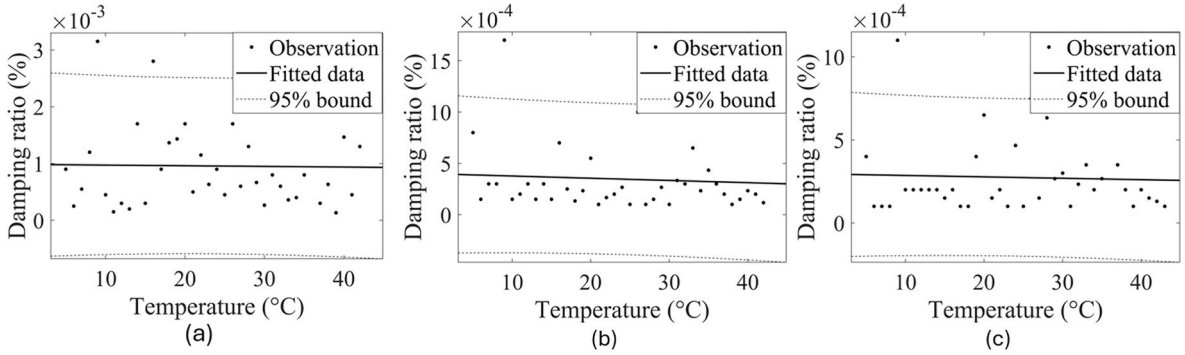

Fig. 9. Relationship between n-order (n = 1,2 and3) a, b, and c, respectively, damping ratio and temperature of the practical results.

4. Simulation analysis on the influence of temperature on the modal parameters

Midas/Civil is a specialized finite-element program used mostly for linear-elastic slight deformation beam element computations in the field of bridge design and general structural analysis. This software was used to simulate the bridge model. The length of the bridge is 610 m, and the span composition is (80 + 3 × 150 + 80) m. This is a two-way bridge. The bridge decks have a full width of 12m, and the maximum height from the ground to the top of the bridge is 127.3 m. A three-dimensional solid-element model of the upstream bridge is created without considering the foundation, and the bridge piers are fixed to the ground. The main span's four piers are fixedly attached to the main box girder, and the two side piers are not fixed to the girder, as shown in Fig. 10. The nodes and elements of the model are 1073 and 1038, respectively. This model has considered two types of materials: concrete and steel. The upper structure of the bridge box girder is a three-directional prestressed concrete structure with a concrete strength class C55, with low-relaxation high-strength steel wires. The central abutment of the lower structure is a double thin-wall hollow pier with a concrete strength class C40.

This study utilized Equation (1) to determine the modulus of elasticity of the materials at different temperatures. The temperature coefficient of the elastic modulus for concrete is 0.003 (Code, 2010), while the temperature coefficient of the elastic modulus for steel, θ_E, is 0.000278, as proposed by (Keulegan and Houseman, 1933).

4.1. Frequency analysis of the simulation results

The natural frequencies of the first three orders of the testing bridge model were determined at a fundamental frequency temperature of 20 °C. The first three-order natural frequency of the testing bridge model was acquired consecutively at −20 °C to 80 °C. Simulation findings of the bridge are described as black points showing a relationship between n-order natural frequency ($n = 1$, 2, and 3) and temperature, as shown in Fig. 11. The equations of the fitted data lines of the first, second, and third natural frequencies are $f_1(T) = -1.31 \times 10^{-3} \times T + 0.9056$, $f_2(T) = -1.86 \times 10^{-3} \times T + 1.289$, and $f_3(T) = -2.01 \times 10^{-3} \times T + 1.393$, respectively, created by linear regression. The temperature coefficients of the first, second, and third frequencies c_1 , c_2 , and c_3 are -1.31×10^{-3}, -1.86×10^{-3}, and -2.01×10^{-3}.

As illustrated in Fig. 11, the relationship between natural frequency and temperature is a negative correlation in the temperature range of −20 °C to 80 °C. As the temperature rises by one °C from 5 °C to 6 °C, the first-order natural frequency of 0.1464% falls. Second-order and third-order natural frequencies show a negative relationship with temperature as well. Reductions in the second-order and third-order frequency are obtained by 0.1457% and 0.145%, respectively, when the temperature increases by 1 °C from 5 °C to 6 °C.

4.2. Mode shape analysis of the simulation results

The testing bridge model's first three modes were found at a fundamental mode shape temperature of 20 °C. At − 20 °C, − 10 °C, 0 °C, 10 °C, 20 °C, 30 °C, 40 °C, 60°Cand 80 °C, the testing bridge model's first three modes were successively recorded as shown in Fig. 12. The bridge's simulation results show n-mode (n = 1, 2, and 3) (a, b, and c), respectively at different temperatures. The effect of temperature on the first mode shape is not remarkable, but the effect of temperature on the second and third mode shapes is very tiny, which is also negligible.

4.3. Damping ratio of the simulation results

The damping ratio of the first three orders of the testing bridge model was determined at a fundamental damping ratio temperature of 20 °C. It

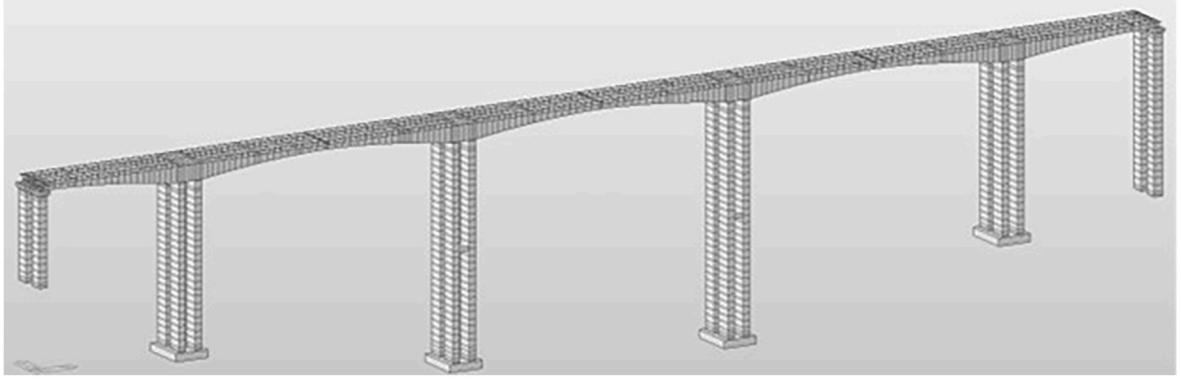

Fig. 10. Simulation model of the observation bridge.

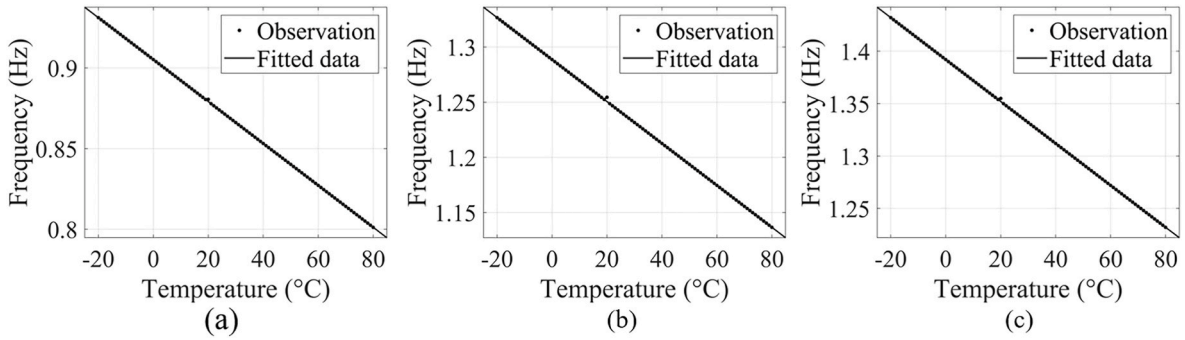

Fig. 11. Relationship between the n-order (1, 2, and 3) a, b, and c, respectively, natural frequency and the temperature of the simulation results.

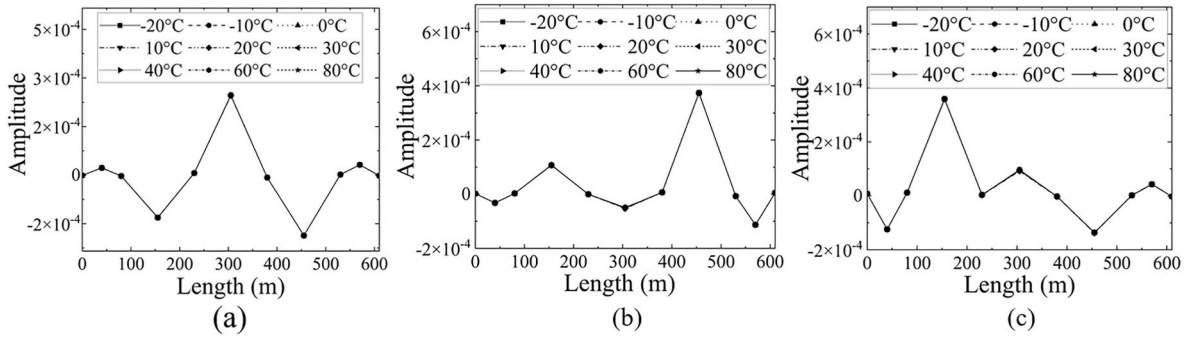

Fig. 12. The simulation results of the first, second, and third modes (a, b, and c), respectively, at different temperatures.

was acquired consecutively at −20 °C to 80 °C. Obtaining a damping ratio is challenging in the simulation analysis of a bridge. However, here is a general procedure for calculating the damping ratio of a bridge in Midas Civil. Midas Civil is a specialized finite element analysis (FEA) software developed by MIDAS IT for the structural analysis and design of bridges and civil engineering structures. It is widely used by engineers to perform complex structural simulations, including static, dynamic, and nonlinear analyses. The result of the modal analysis gives the natural frequencies and mode shapes of the structure, and the damping ratio is often derived from the results natural frequency of this analysis. A step-by-step process was followed to obtain the simulation damping ratio from Midas Civil. 1. Fixed frequencies f_1 and f_{17}; 2. Converted to angular frequencies ω_1 and ω_2; 3. Replace the Rayleigh damping formula (Formula (12-16)) to calculate (α and β); 4. The damping ratio of each order (ζ_n) is calculated based on Equation (12). The Rayleigh Damping method also required the first frequency and a higher frequency as reference.

Applying the formula for the damping ratio is obtained from the article (Semblat, 1997):

$$\zeta_n = \frac{1}{2}\left(\frac{\alpha}{\omega_n} + \beta\omega_n\right), \tag{12}$$

where ζ_n is n order Damping ratios, α and β are Rayleigh damping coefficients, and ω_n is n order angular frequencies.

$$\zeta = \frac{1}{2}\left(\frac{\alpha}{\omega_1} + \beta\omega_1\right), \tag{13}$$

$$\zeta = \frac{1}{2}\left(\frac{\alpha}{\omega_2} + \beta\omega_2\right), \tag{14}$$

solve for (α and β) came from equation (13) and equation (14)

$$\alpha = \frac{2\zeta(\omega_1\omega_2)}{\omega_2 + \omega_1}, \tag{15}$$

$$\beta = \frac{2\zeta}{\omega_2 + \omega_1}, \tag{16}$$

where ζ is (0.05) damping ratio and ω_1 *and* ω_2 *are* the first frequency and the (17th) frequency respectively as references.

The points are described as observations of the damping ratio, and equations of the fitted lines of the first, second, and third damping ratios are $\zeta_1(T) = 0 \times T + 0.05$, $\zeta_2(T) = 0 \times T + 0.0404$, and $\zeta_3(T) = 0 \times T + 0.039$, respectively, have been created by linear regression, as shown in Fig. 13. The temperature coefficients of the first, second, and third damping ratios c_1, c_2, and c_3 are 0, 0, and 0. The fitted lines show that temperature has no correlation to the damping ratio, as shown in Fig. 13 in the temperature range of −20 °C–80 °C. As the temperature rises by one °C from 5 °C to 6 °C, Changes in first, second, and third-order damping ratios are 0 %.

5. Discussion

5.1. Frequency

The results of Table 1 prove that the relationship between the n-order natural frequency ($n = 1$, 2, and 3) and temperature of the testing result and simulation results is compatible with each other; the correlation coefficients of the n-order frequency and temperature of practical data are -1.85×10^{-3}, -1.83×10^{-3}, and -2.01×10^{-3}, and the correlation coefficients of the n-order frequency and temperature of simulation data are -1.31×10^{-3}, -1.86×10^{-3}, and -2.01×10^{-3}.

So, the Absolute error between the results of two types of analysis—finite element and practical—is very little: 5.4×10^{-4}, 3.0×10^{-5}, and 0.00 for the first, second, and third-order natural frequencies, respectively. Fig. 14 shows that practical and simulation results fit each other; temperature has a negative correlation to the natural frequency of a continuous rigid-frame bridge, and it should be considered when identifying the bridge's health. This result is from FE analysis and (39)

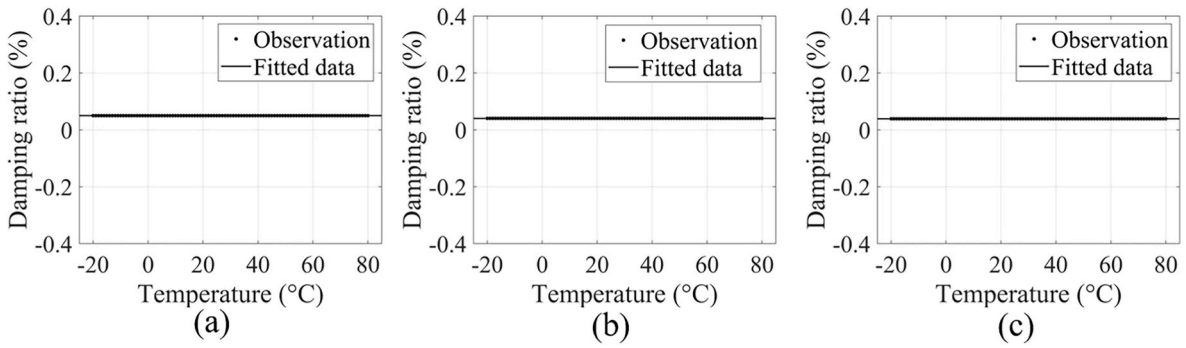

Fig. 13. Relationship between the n-order (1, 2, and 3) a, b, and c, respectively, damping ratio and temperature of the simulation results.

Table 1
Regression coefficients of frequency.

Coefficient	Practical	Simulation	|Absolute error|
c_1	-1.85×10^{-3}	-1.31×10^{-3}	5.4×10^{-4}
c_2	-1.83×10^{-3}	-1.86×10^{-3}	3.0×10^{-5}
c_3	-2.01×10^{-3}	-2.01×10^{-3}	0

practical tests analysis. Additionally, a large amount of tests may provide more accurate results in future studies.

5.2. Mode shape

In simulation results, the first mode shape is not significantly affected by temperature, but the second and third mode shapes are likewise negligibly affected as shown in Fig. 12 which are almost identical at different temperatures. The practical results described the mode shape, as shown in Fig. 8. There is no temperature influence on the first mode shape, as illustrated in Fig. 8 (a) at temperatures of 15 °C, 25 °C, and 43 °C. Furthermore, there are minimal variations at 10 °C, 20 °C, and 30 °C; this could be an error. At temperatures 10 °C, 20 °C, 25 °C, 30 °C, and 43 °C, the second and third mode shape provide distinct outcomes. Thus, as illustrated in Fig. 8(b) and (c), it demonstrated that the second and third mode shapes may have a temperature influence. Because each mode shape is different at different temperatures.

However, in real practice, defining the mode shape of massive structures with complex boundary conditions is difficult, the findings might not be entirely correct; For several reasons: 1. A large Size of the bridge varies the dynamic responses. 2. As a highway bridge, the traffic load is not always the same during the various data measurements; 3. Changes in boundary conditions brought on by environmental factors may have an impact on mode shape; 5. Data preparation methods filtering, denoising, and mode shape identification algorithms. Therefore, it is challenging to claim the temperature effect on the mode shape of a structure. This result is from FE analysis and limited practical tests analysis. A large number of tests could provide more accurate results of the temperature effect on the mode shape of a large bridge in future studies.

5.3. Amping ratio

The results of Table 2 demonstrate that the relationship between the n-order ($n = 1$, 2, and 3) damping ratio and temperature of the testing result and simulation results are compatible with each other; the correlation coefficients of the n-order damping ratio and temperature of practical data are -1.14×10^{-6}, -2.1×10^{-6}, and -8.4×10^{-7}, and the correlation coefficients of the n-order damping ratio and temperature of simulation data are 0, 0, and 0. So, the absolute error between the results of two types of analysis—finite element and practical—is very little: 1.14×10^{-6}, 2.1×10^{-6}, and 8.4×10^{-7} for the first, second, and third-order damping ratios, respectively. Fig. 15 shows that temperature has no significant correlation to the damping ratio of a continuous rigid-frame bridge in this study. So it may be negligible. However, to get the conclusion of the temperature effect on damping ratios a large amount of data is required.

However, the relative errors of simulation and practical damping ratios remain high due to the challenges in accurately identifying the damping ratio from both simulation and practical data. This finding represents a primary contribution of the research in the context of finite element analysis (FEA) and practical testing. A large number of tests and

Table 2
Regression coefficients of damping ratio.

Coefficient	Practical	Simulation	|Absolute error|
c_1	-1.14×10^{-6}	0	1.14×10^{-6}
c_2	-2.1×10^{-6}	0	2.1×10^{-6}
c_3	-8.4×10^{-7}	0	8.4×10^{-7}

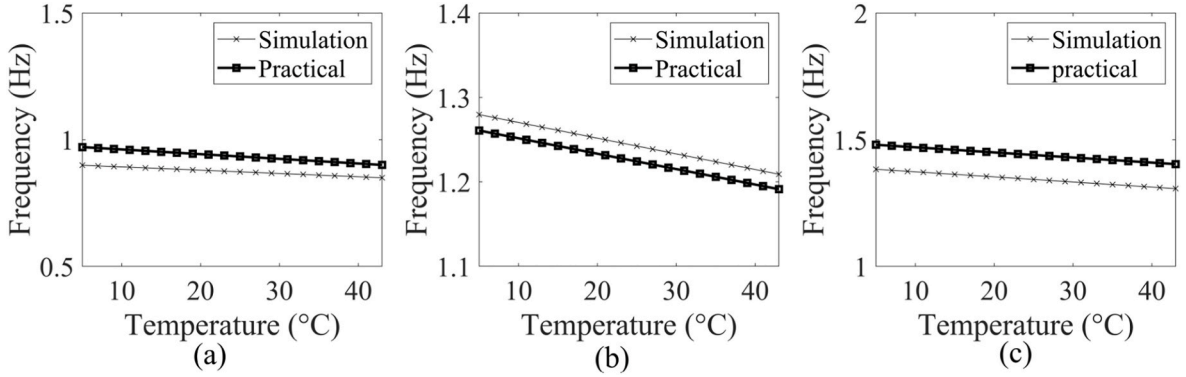

Fig. 14. Relationship between the n-order natural frequency ($n = 1$, 2, and 3) a, b, and c, respectively, and temperature of the testing and simulation results.

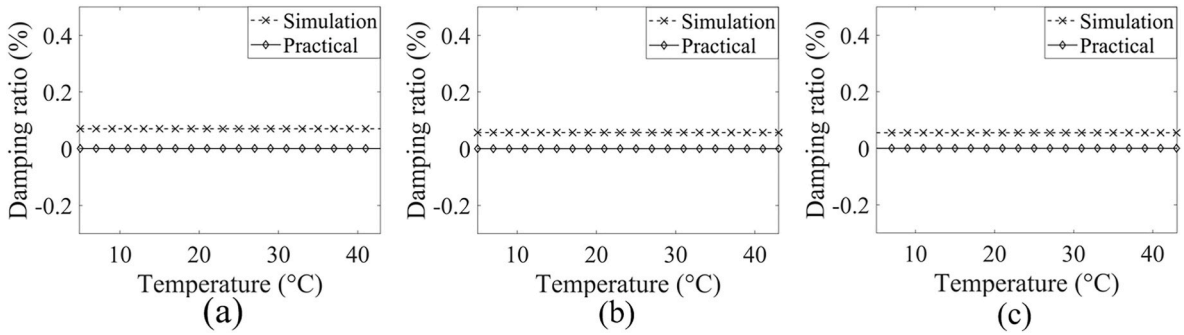

Fig. 15. Relationship between n-mode (n = 1,2 and3) a, b, and c, respectively, damping ratio and temperature of the practical and simulation results.

new damping ratio identification methods of a large bridge could provide more precise results in future studies.

6. Conclusion

The impact of temperature on modal characteristics like natural frequencies, mode shapes, and damping ratios is essential for accurately assessing a bridge's condition. This research presents the findings of a one-year limited to 39 tests due to constraints such as the regional temperature range in Chongqing, China (5 °C–43 °C annually). And findings with finite element (FE) analysis over a broader temperature range (−20 °C–80 °C), yielding a total of 101 datasets. The study investigates the effect of temperature on the modal parameters of a large continuous rigid-frame bridge. The results of the experiment and FE analysis lead to the following conclusions:

Temperature plays a crucial role in affecting the frequency of a continuous rigid-frame bridge. Specifically, as the temperature of the bridge increases from winter to summer, its frequency decreases. There exists a negative correlation between frequency and temperature. Furthermore, the impact of temperature on frequency is more pronounced than its influence on the damping ratio and mode shapes.

The study demonstrates that the effect of temperature is negligible for the first mode shape of the continuous rigid-frame bridge. However, the temperature may influence the second and third-mode shapes, although this effect is minimal. Additionally, it is challenging to claim the temperature effect on the mode shapes of large bridges with limited data sets, It requires broad testing to achieve a precise finding about how temperature affects a large structure's mode shapes.

Temperature has no considerable relation to the damping ratio of the continuous rigid-frame bridge. It is a summary of the FE analysis and (39) practical tests analysis. Additionally, A large number of tests might provide more accurate results of the temperature effect on the damping ratios of a large bridge in future studies.

Vibration-based identification methods can effectively be applied to assess bridge conditions, and it is essential to define various modal parameters, particularly the frequency changes by environmental factors, especially temperature. Without a good understanding of temperature effects poses challenges in accurately determining the health status of a bridge.

CRediT authorship contribution statement

Yang Yang: Project administration, Methodology, Investigation, Funding acquisition, Conceptualization. **Md Sulayman Hossen:** Writing – original draft, Formal analysis, Data curation. **Giuseppe Lacidogna:** Writing – review & editing, Validation, Supervision. **Wenming Xu:** Writing – original draft, Methodology, Investigation. **Ibna Kawsar:** Validation, Software. **Junbo Sun:** Writing – review & editing. **Shameem Hossain:** Formal analysis, Data curation.

Declaration of competing interest

The authors declared that they have no conflicts of interest to this work.

We declare that we do not have any commercial or associative interest that represents a conflict of interest in connection with the work submitted.

Acknowledgments

We are grateful to the following agencies for supporting this study: Research Project of Zhejiang Provincial Department of Transportation-Intelligent Detection Method for Mechanical Indicators of Bridge Structures ZJPDT-IDMMIBS, Innovation Group Project of the National Natural Science Foundation of China 52221002, Fundamental Research Funds for the Central Universities of China 2022CDJQY-009.

Data availability

Data will be made available on request.

References

Abdal, S., et al., 2023. Application of ultra-high-performance concrete in bridge engineering: current status, limitations, challenges, and future prospects. Buildings 13 (1). https://doi.org/10.3390/buildings13010185.

Akbari, R., Maadani, S., Maalek, S., 2018. On the fundamental natural frequency of bridge decks: review and applications. Proc. Inst. Civ. Eng. Build. 171 (12), 931–945.

Asadollahi, P., Li, J., 2017. Statistical analysis of modal properties of a cable-stayed bridge through long-term wireless structural health monitoring. J. Bridge Eng. 22 (9), 1–15. https://doi.org/10.1061/(asce)be.1943-5592.0001093.

Bai, Y., et al., 2023. Research on steel structure damage detection based on TCD-CNN method. Structures 57 (September), 105318. https://doi.org/10.1016/j.istruc.2023.105318.

Borlenghi, P., Saisi, A., Gentile, C., 2024. Vibration monitoring of masonry bridges to assess damage under changing temperature. Dev. Built Environ. 20 (September), 100555. https://doi.org/10.1016/j.dibe.2024.100555.

Brownjohn, J.M.W., De Stefano, A., Xu, Y.-L., Wenzel, H., Aktan, A.E., 2011. Vibration-based monitoring of civil infrastructure: challenges and successes. J. Civ. Struct. Heal. Monit. 1, 79–95.

Cai, Y., Zhang, K., Ye, Z., Liu, C., Lu, K., Wang, L., 2021. Influence of temperature on the natural vibration characteristics of simply supported reinforced concrete beam. Sensors 21 (12). https://doi.org/10.3390/s21124242.

Chalouhi, E.K., Gonzalez, I., Gentile, C., Karoumi, R., 2018. Vibration-based SHM of railway bridges using machine learning: the influence of temperature on the health prediction. In: Experimental Vibration Analysis for Civil Structures: Testing, Sensing, Monitoring, and Control 7. Springer, pp. 200–211.

Code, M., 2010. FIB. Special Activity Group 5. CEB and FIB.

Dang, V.-H., Vu, T.-C., Nguyen, B.-D., Nguyen, Q.-H., Nguyen, T.-D., 2022. Structural damage detection framework based on graph convolutional network directly using vibration data. In: Structures. Elsevier, pp. 40–51.

De Luca, A., Bauer, M., Pinto, M., Malsch, E., 2018. Vibration analysis of footbridges: an overview of the current practice. MATEC Web Conf. 211, 1–9. https://doi.org/10.1051/matecconf/201821110002.

Doyle, J.F., 1991. Static and dynamic analysis of structures. With an emphasis on mechanics and computer matrix methods. Solid Mechanics and its Applications Series, Springer Dordrecht XIV, 442.

He, X., Tan, G., Chu, W., Zhang, S., Wei, X., 2022. Reliability assessment method for simply supported bridge based on structural health monitoring of frequency with

temperature and humidity effect eliminated. Sustain. Times 14 (15). https://doi.org/10.3390/su14159600.
Keulegan, G.H., Houseman, M.R., 1933. Temperature coefficient of the moduli of metals and alloys used as elastic elements. Bur. Stand. J. Res. 10 (3), 289. https://doi.org/10.6028/jres.010.022.
Kim, J.-T., Park, J.-H., Lee, B.-J., 2007. Vibration-based damage monitoring in model plate-girder bridges under uncertain temperature conditions. Eng. Struct. 29 (7), 1354–1365.
Liu, Y., 2023. Research on bridge damage identification method based on dynamic characteristics. J. Eng. Res. Reports 25 (8), 87–93. https://doi.org/10.9734/jerr/2023/v25i8961.
Luo, J., Huang, M., Lei, Y., 2022. Temperature effect on vibration properties and vibration-based damage identification of bridge structures: a literature review. Buildings 12 (8). https://doi.org/10.3390/buildings12081209.
Magalhães, F., Cunha, Á., Caetano, E., 2009. One-year dynamic monitoring of a bridge: modal parameters tracking under the influence of environmental effects. In: Struct. Heal. Monit. Intell. Infrastruct. - Proc. 4th Int. Conf. Struct. Heal. Monit. Intell. Infrastructure, SHMII 2009. July.
Mekjavić, I., 2013. Damage identification of bridges from vibration frequencies. Teh. Vjesn. 20 (1), 155–160.
Mosavi, A.A., Seracino, R., Rizkalla, S., 2012. Effect of temperature on daily modal variability of a steel-concrete composite bridge. J. Bridge Eng. 17 (6), 979–983. https://doi.org/10.1061/(asce)be.1943-5592.0000372.
Moughty, J.J., Casas, J.R., 2017. A state of the art review of modal-based damage detection in bridges: development, challenges, and solutions. Appl. Sci. 7 (5). https://doi.org/10.3390/app7050510.
Salawu, O.S., 1997. Detection of structural damage through changes in frequency: a review. Eng. Struct. 19 (9), 718–723.
Semblat, J.F., 1997. Rheological interpretation of Rayleigh damping. J. Sound Vib. 206 (5), 741–744. https://doi.org/10.1006/jsvi.1997.1067.
Shan, W., Wang, X., Jiao, Y., 2018. Modeling of temperature effect on modal frequency of concrete beam based on field monitoring data. Shock Vib. 2018. https://doi.org/10.1155/2018/8072843.
Shi, Z., Hong, Y., Yang, S., 2019. Updating boundary conditions for bridge structures using modal parameters. Eng. Struct. 196, 109346.
Wang, L., Hou, J., Ou, J., 2011. Temperature effect on modal frequencies for a rigid continous bridge based on long term monitoring. Nondestruct. Charact. Compos. Mater. Aerosp. Eng. Civ. Infrastructure, Homel. Secur. 2011 7983 (April 2011), 79830I. https://doi.org/10.1117/12.880430.
Wang, Z., Huang, M., Gu, J., 2020. Temperature effects on vibration-based damage detection of a reinforced concrete slab. Appl. Sci. 10 (8). https://doi.org/10.3390/app10082869.
Warburton, G.B., 1995. In: Clough, Ray W., Penzien, Joseph (Eds.), Dynamics of Structures. Wiley Online Library, McGraw-Hill, New York, p. 738. ISBN 0-07-011394-7.
Xia, Y., Chen, B., Weng, S., Ni, Y.Q., Xu, Y.L., 2012. Temperature effect on vibration properties of civil structures: a literature review and case studies. J. Civ. Struct. Heal. Monit. 2 (1), 29–46. https://doi.org/10.1007/s13349-011-0015-7.
Xia, Q., Wu, W., Li, F., Zhou, X., Xu, Y., Xia, Y., 2022. Temperature behaviors of an arch bridge through integration of field monitoring and unified numerical simulation. Adv. Struct. Eng. 25 (16), 3492–3509.
Xu, Y., Zhu, S., Zong, Z., 2007. Experimental study on effects of environmental temperature on dynamic characteristics of bridge structures. Earthq. Eng. Eng. Vib. Ed. 27 (6), 119.
Zhu, J., Zhang, C., Li, X., 2023. Structural damage detection of the bridge under moving loads with the quasi-static displacement influence line from one sensor. Meas. J. Int. Meas. Confed. 211 (February), 112599. https://doi.org/10.1016/j.measurement.2023.112599.